Electronic Supplementary Material (ESI) for Dalton Transactions.

POM Species, Temperature and Counterions Modulated the Various Dimensionalities of POM-based Metal-Organic Frameworks

Jing-Wen Sun,[†] Peng-Fei Yan,[*,†] Guang-Hui An,[†] Jing-Quan Sha,[‡] Cheng Wang,[†] and Guang-Ming Li[*,†]

[†]*Key Laboratory of Functional Inorganic Material Chemistry (MOE), P. R. China; School of Chemistry and Materials Science, Heilongjiang University; Harbin, 150080, P. R. China*

[‡]*School of Pharmacy, Jiamusi University, Jiamusi, 154007, P. R. China*

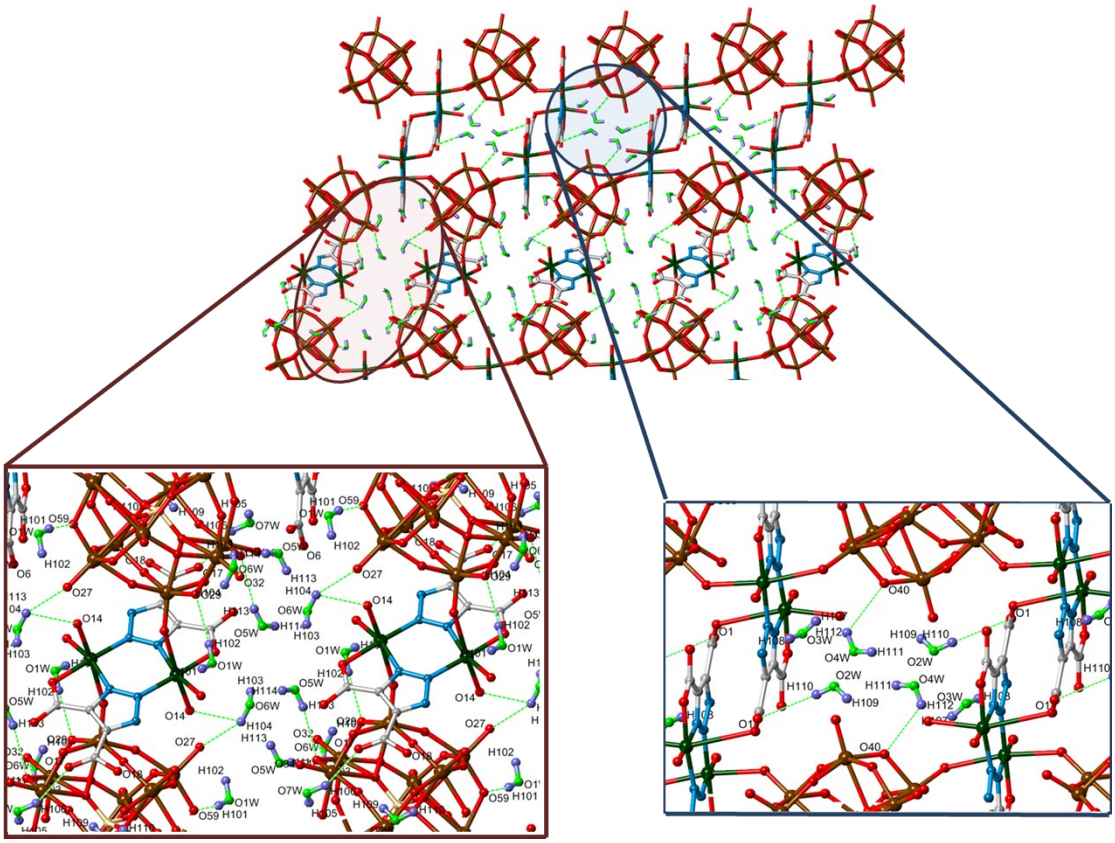

Figure S1. The interactions between water molecules, 2D POM-SBU layers in **2**.

Table S1. Bond lengths [Å] and angles [deg] for **2**

D–H···A	d(D–H) (Å)	d(H···A) (Å)	D–H···A (deg)
O(1W)–H(102)···O(29)	0.849	2.208	171.719
O(1W)–H(101)···O(59)	0.855	2.222	169.680
O(2W)–H(110)···O(1)	0.828	2.748	166.706
O(4W)–H(112)···O(40)	0.849	2.588	122.031
O(5W)–H(113)···O(29)	0.828	2.337	167.130
O(6W)–H(103)···O(32)	0.834	2.767	120.194
O(6W)–H(104)···O(27)	0.860	2.574	147.782
O(7W)–H(106)···O(17)	0.867	2.105	151.285

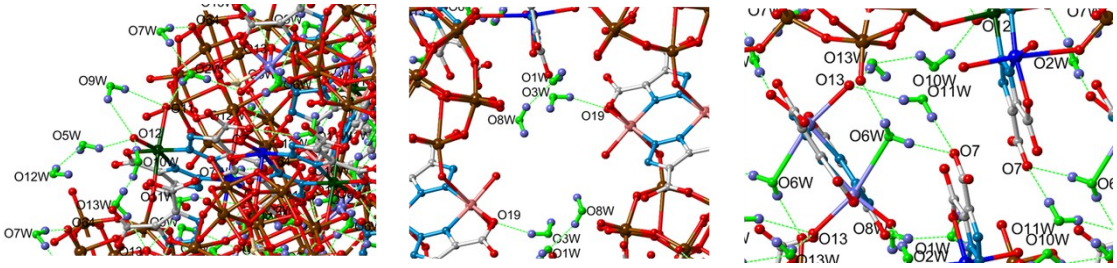

Figure S2. The H-bond interactions in **3**.

Table S2. Bond lengths [Å] and angles [deg] for **3**

D–H···A	d(D–H) (Å)	d(H···A) (Å)	D–H···A (deg)
O(1W)–H(118)···O(20)	0.850	2.460	128.386
O(2W)–H(119)···O(14)	0.851	1.854	173.307
O(2W)–H(120)···O(11)	0.851	2.031	165.269
O(3W)–H(501)···O(19)	0.858	2.167	162.709
O(5W)–H(125)···O(12)	0.851	1.998	151.276
O(6W)–H(123)···O(7)	0.849	1.982	154.941
O(6W)–H(124)···O(62)	0.851	2.485	166.406
O(7W)–H(122)···O(2W)	0.850	2.014	165.545
O(7W)–H(121)···O(64)	0.851	2.112	168.731
O(8W)–H(116)···O(1W)	0.850	1.933	156.621
O(9W)–H(113)···O(11)	0.851	2.451	166.116
O(9W)–H(114)···O(12)	0.849	2.395	129.194
O(10W)–H(112)···O(13W)	0.851	2.032	119.858
O(10W)–H(111)···O(10)	0.850	1.804	152.481
O(11W)–H(109)···O(13)	0.851	2.313	149.344
O(11W)–H(110)···O(7)	0.848	2.447	148.196
O(12W)–H(101)···O(5W)	0.850	2.100	138.888
O(13W)–H(103)···O(13)	0.851	2.002	158.198

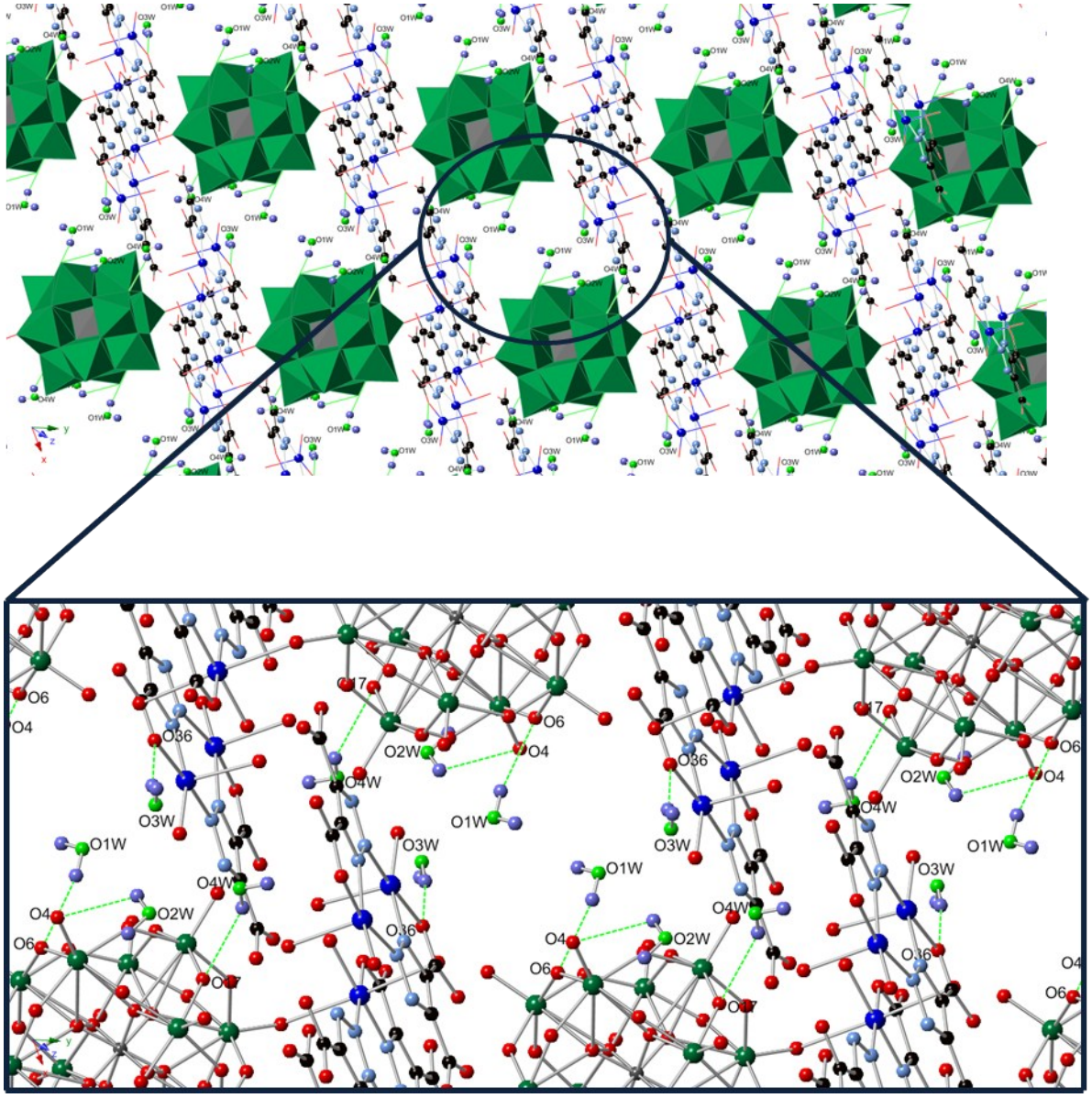

Figure S3. The H-bond interactions in **4**.

Table S3. Bond lengths [Å] and angles [deg] for **4**

D–H···A	d(D–H) (Å)	d(H···A) (Å)	D–H···A (deg)
O(1W)–H(101)···O(6)	0.849	2.405	167.174
O(2W)–H(103)···O(4)	0.855	2.772	125.358
O(3W)–H(105)···O(36)	0.847	2.345	168.685
O(4W)–H(107)···O(17)	0.853	2.772	149.274

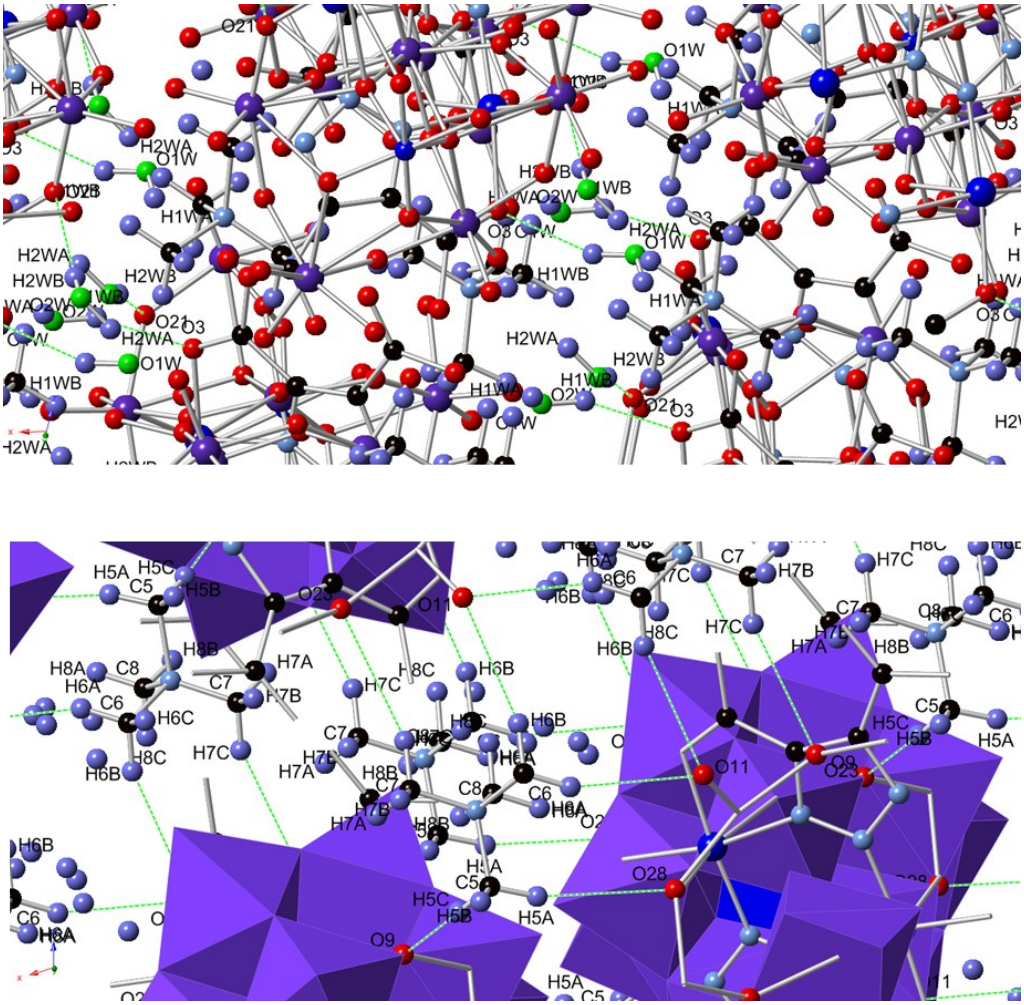

Figure S4. The H-bond interactions in **5**.

Table S4. Bond lengths [Å] and angles [deg] for **5**

D–H···A	d(D–H) (Å)	d(H···A) (Å)	D–H···A (deg)
O(1W)–H(1WB)··O(3)	0.851	2.087	156.581
O(2W)–H(2WB)··O(21)	0.845	2.789	171.299
C(5)–H(5A)···O(28)	0.956	2.686	165.737
C(5)–H(5C)···O(9)	0.956	2.686	165.737
C(6)–H(6A)···O(11)	0.951	2.564	152.513
C(6)–H(6B)···O(11)	0.969	2.724	149.372
C(7)–H(7C)···O(23)	0958	2.799	157.148

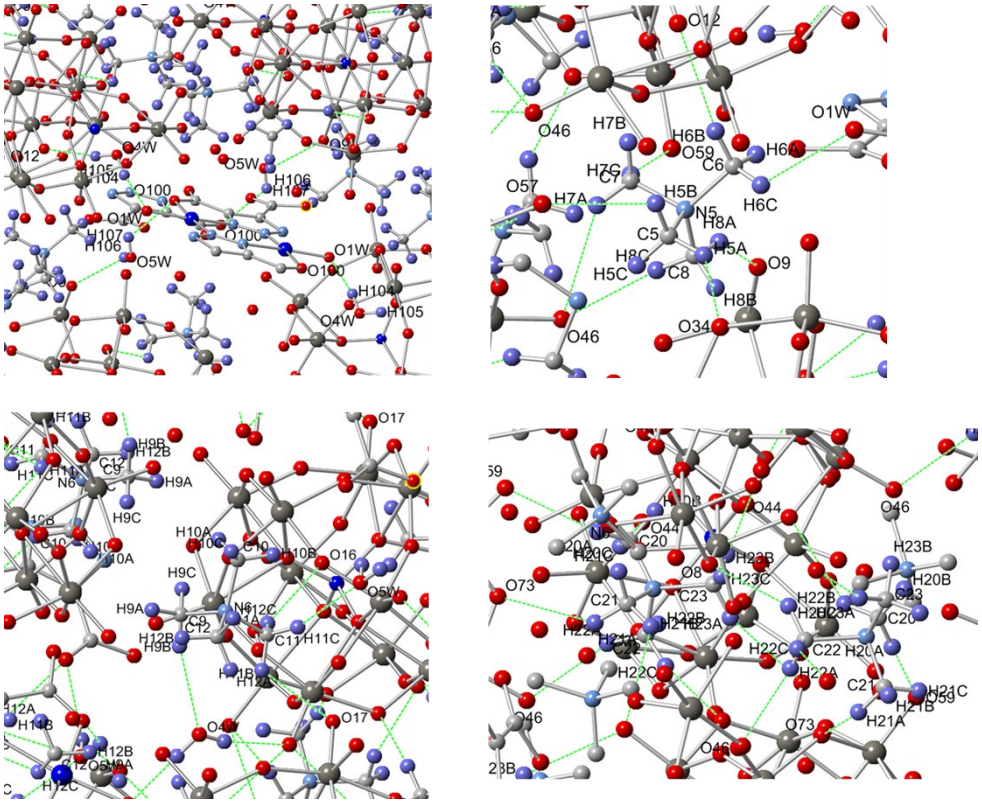

Figure S5. The H-bond interactions in **6**.

Table S5. Bond lengths [Å] and angles [deg] for **6**

D–H···A	d(D–H) (Å)	d(H···A) (Å)	D–H···A (deg)
O(5W)–H(107)··O(100)	0.849	2.660	127.845
O(5W)–H(106)··O(9)	0.854	2.455	121.546
O(4W)–H(106)···O(12)	0.850	2.068	168.743
O(4W)–H(104)···O(1W)	0.845	1.869	160.773
C(5)–H(5A)···O(34)	0.960	2.484	133.947
C(5)–H(5B)···O(57)	0.964	2.746	132.898
C(6)–H(6C)···O(1W)	0.963	2.731	126.416
C(6)–H(6B)···O(12)	0.962	2.543	145.217
C(7)–H(7A)···O(46)	0.961	2.796	130.047
C(7)–H(7C)···O(59)	0.963	2.615	158.260
C(8)–H(8C)···O(46)	0.963	2.352	155.884
C(8)–H(8A)···O(9)	0.959	2.346	145.147
C(9)–H(9B)···O(4W)	0.957	2.678	165.748
C(11)–H(11B)···O(17)	0.967	2.455	117.079
C(11)–H(11C)···O(5W)	0.954	2.541	160.240
C(11)–H(11A)···O(16)	0.960	2.692	139.490
C(22)–H(22B)···O(8)	0.954	2.439	143.649
C(22)–H(22A)···O(46)	0.968	2.414	156.965
C(20)–H(20A)···O(59)	0.963	2.538	156.116
C(21)–H(21A)···O(73)	0.956	2.748	135.701
C(23)–H(23A)···O(44)	0.963	2.669	146.424

Table S6. Selected bond lengths [Å] and angles [deg] for **1**

N(4)-Cu(2)	1.91(3)	N(1)-Cu(4)	2.02(3)
N(6)-Cu(1)	2.00(3)	O(21)-Cu(3)	2.42(2)
N(7)-Cu(1)	1.95(3)	O(32)-Cu(3)	1.90(3)
N(10)-Cu(3)	1.97(2)	O(35)-Cu(1)	2.02(3)
N(11)-Cu(3)	2.01(3)	O(36)-Cu(1)	2.25(3)
N(8)-Cu(4)	1.94(3)	O(42)-Cu(2)	1.95(2)
N(2)-Cu(2)	1.95(3)	O(43)-Cu(1)	2.40(2)
O(55)-Cu(1)	2.09(3)	O(50)-Cu(2)	1.97(2)
O(57)-Cu(4)	2.00(3)	O(51)-Cu(4)	2.41(3)
O(63)-Cu(4)	1.95(3)	O(63)-Cu(4)-O(57)	92.5(15)
O(32)-Cu(3)-N(11)	171.6(11)	N(10)-Cu(3)-N(11)	95.2(9)
N(7)-Cu(1)-N(6)	97.1(11)	O(17)-Cu(3)-N(11)	83.1(11)
N(7)-Cu(1)-O(35)	175.0(12)	O(32)-Cu(3)-O(21)	91.2(10)
N(6)-Cu(1)-O(35)	79.0(12)	N(10)-Cu(3)-O(21)	87.9(9)
N(7)-Cu(1)-O(55)	94.1(13)	O(17)-Cu(3)-O(21)	93.9(9)
N(6)-Cu(1)-O(55)	166.5(14)	N(11)-Cu(3)-O(21)	94.3(8)
O(35)-Cu(1)-O(55)	89.4(14)	N(8)-Cu(4)-O(63)	176.4(13)
N(7)-Cu(1)-O(36)	92.9(13)	N(8)-Cu(4)-O(57)	86.6(13)
N(6)-Cu(1)-O(36)	96.4(13)	N(10)-Cu(3)-O(17)	177.6(11)
O(35)-Cu(1)-O(36)	90.6(13)	N(8)-Cu(4)-N(1)	97.1(12)
O(55)-Cu(1)-O(36)	90.5(14)	O(63)-Cu(4)-N(1)	83.5(14)
N(7)-Cu(1)-O(43)	86.2(10)	O(57)-Cu(4)-N(1)	173.8(15)
N(6)-Cu(1)-O(43)	88.7(10)	N(8)-Cu(4)-O(51)	91.9(11)
O(35)-Cu(1)-O(43)	90.6(9)	O(63)-Cu(4)-O(51)	91.7(12)
O(55)-Cu(1)-O(43)	84.6(12)	O(57)-Cu(4)-O(51)	93.5(13)
O(36)-Cu(1)-O(43)	174.9(11)	N(1)-Cu(4)-O(51)	91.3(12)
N(4)-Cu(2)-N(2)	95.6(10)	N(4)-Cu(2)-O(50)	171.9(10)
N(4)-Cu(2)-O(42)	89.9(10)	N(2)-Cu(2)-O(50)	81.9(10)
N(2)-Cu(2)-O(42)	174.4(12)	O(42)-Cu(2)-O(50)	92.5(10)
O(32)-Cu(3)-O(17)	90.2(13)	O(32)-Cu(3)-N(10)	91.3(13)

Table S7. Selected bond lengths [Å] and angles [deg] for **2**

N(1)-Cu(2)	1.969(5)	O(10)-Cu(3)	2.373(5)
N(2)-Cu(3)	1.936(5)	O(11)-Cu(3)	1.951(5)
N(8)-Cu(1)	1.966(6)	O(13)-Cu(1)	1.947(5)
O(4)-Cu(3)	1.968(5)	O(14)-Cu(1)	2.314(5)
O(8)-Cu(2)	1.978(4)	O(15)-Cu(1)#1	1.962(6)
O(9)-Cu(2)	1.932(5)	O(15)#1-Cu(1)-O(14)	87.6(2)
O(13)-Cu(1)-O(15)#1	88.1(3)	N(8)-Cu(1)-O(14)	94.9(2)
O(13)-Cu(1)-N(8)	92.6(3)	N(7)#1-Cu(1)-O(14)	94.3(2)
O(15)#1-Cu(1)-N(8)	177.3(2)	O(9)-Cu(2)-N(5)	91.5(2)
O(13)-Cu(1)-N(7)#1	165.8(2)	O(9)-Cu(2)-N(1)	171.2(2)
O(15)#1-Cu(1)-N(7)#1	81.7(3)	N(5)-Cu(2)-N(1)	97.2(2)
N(8)-Cu(1)-N(7)#1	97.2(2)	O(9)-Cu(2)-O(8)	89.6(2)
O(13)-Cu(1)-O(14)	95.2(3)	N(5)-Cu(2)-O(8)	178.9(2)
N(1)-Cu(2)-O(8)	81.6(2)	O(11)-Cu(3)-O(4)	88.5(2)
N(2)-Cu(3)-O(11)	92.4(2)	N(6)-Cu(3)-O(4)	81.8(2)
N(2)-Cu(3)-N(6)	96.9(2)	N(2)-Cu(3)-O(10)	100.76(19)
O(11)-Cu(3)-N(6)	169.8(2)	O(11)-Cu(3)-O(10)	95.7(2)
N(2)-Cu(3)-O(4)	173.1(2)	N(6)-Cu(3)-O(10)	86.7(2)
O(4)-Cu(3)-O(10)	86.00(19)		

Symmetry transformations used to generate equivalent atoms: #1 -x+1, -y+2, -z+2.

Table S8. Selected bond lengths [Å] and angles [deg] for **3**

Cu(1)-N(2)	1.933(6)	Cu(2)-O(11)	2.348(6)
Cu(1)-O(9)	1.957(6)	Cu(4)-N(11)	1.959(7)
Cu(1)-O(5)	1.972(6)	Cu(4)-N(10)#2	1.976(7)
Cu(1)-N(4)	1.975(7)	Cu(4)-O(24)	1.977(6)
Cu(1)-O(10)	2.254(7)	Cu(4)-O(19)	1.989(5)
Cu(2)-O(12)	1.955(6)	Cu(4)-O(21)	2.247(7)
Cu(2)-N(3)#1	1.969(7)	O(1)-Cu(2)#3	2.007(6)
Cu(2)-N(5)#1	1.990(7)	N(3)-Cu(2)#3	1.969(7)
Cu(2)-O(1)#1	2.007(6)	N(5)-Cu(2)#3	1.990(7)
N(7)-Cu(3)#4	1.961(6)	N(10)-Cu(4)#2	1.976(6)
N(2)-Cu(1)-O(9)	89.0(3)	N(8)-Cu(3)-N(7)#4	97.1(2)
N(2)-Cu(1)-O(5)	170.2(3)	O(12)-Cu(2)-N(3)#1	166.5(3)
O(9)-Cu(1)-O(5)	90.6(2)	O(12)-Cu(2)-N(5)#1	93.1(3)
N(2)-Cu(1)-N(4)	96.3(3)	N(3)#1-Cu(2)-N(5)#1	96.7(3)
O(9)-Cu(1)-N(4)	165.2(3)	O(12)-Cu(2)-O(1)#1	89.2(3)
O(5)-Cu(1)-N(4)	81.8(2)	N(3)#1-Cu(2)-O(1)#1	80.8(3)
N(2)-Cu(1)-O(10)	98.2(3)	N(5)#1-Cu(2)-O(1)#1	177.5(3)
O(9)-Cu(1)-O(10)	97.4(3)	O(12)-Cu(2)-O(11)	92.7(3)
O(5)-Cu(1)-O(10)	91.6(3)	N(3)#1-Cu(2)-O(11)	96.2(2)

N(4)-Cu(1)-O(10)	95.6(3)	N(5)#1-Cu(2)-O(11)	91.8(3)
O(1)#1-Cu(2)-O(11)	89.0(2)	O(14)-Cu(3)-O(18)	87.5(2)
N(11)-Cu(4)-N(10)#2	95.9(3)	N(8)-Cu(3)-O(18)	175.1(3)
N(11)-Cu(4)-O(24)	92.4(3)	N(7)#4-Cu(3)-O(18)	81.9(2)
N(10)#2-Cu(4)-O(24)	161.9(3)	O(14)-Cu(3)-O(13)	96.8(3)
N(11)-Cu(4)-O(19)	173.8(3)	N(8)-Cu(3)-O(13)	89.5(3)
N(10)#2-Cu(4)-O(19)	81.4(2)	N(7)#4-Cu(3)-O(13)	94.9(3)
O(24)-Cu(4)-O(19)	88.8(2)	O(18)-Cu(3)-O(13)	95.3(3)
N(11)-Cu(4)-O(21)	94.3(3)	O(24)-Cu(4)-O(21)	91.4(3)
N(10)#2-Cu(4)-O(21)	104.0(3)	O(19)-Cu(4)-O(21)	91.7(3)
O(14)-Cu(3)-N(7)#4	164.8(3)	O(14)-Cu(3)-N(8)	92.5(3)

Symmetry transformations used to generate equivalent atoms: #1 x-1, y, z; #2 -x-1, -y-1, -z; #3 x+1, y, z; #4 -x, -y-1, -z+1.

Table S9. Selected bond lengths [Å] and angles [deg] for **4**

N(1)-Cu(1)	2.005(9)	N(9)-Cu(1)	1.955(9)
N(2)-Cu(2)	1.962(9)	O(4)-Cu(1)	1.972(8)
N(4)-Cu(2)	1.999(10)	O(5)-Cu(1)	2.278(10)
N(5)-Cu(3)#1	1.973(10)	O(6)-Cu(1)	1.960(9)
N(6)-Cu(3)	1.979(11)	O(7)-Cu(2)	2.312(10)
O(44)-Cu(3)	1.982(9)	O(8)-Cu(2)	1.987(8)
O(14)-Cu(3)	1.951(9)	O(41)-Cu(2)	1.95(2)
O(15)-Cu(3)	2.424(11)	Cu(3)-N(5)#1	1.973(10)
N(1)-Cu(1)-O(5)	96.5(4)	O(41)-Cu(2)-O(8)	88.4(6)
O(41)-Cu(2)-N(2)	93.3(6)	N(2)-Cu(2)-O(8)	174.0(4)
N(9)-Cu(1)-O(6)	95.5(4)	O(4)-Cu(1)-N(1)	81.6(3)
N(9)-Cu(1)-O(4)	166.9(4)	N(9)-Cu(1)-O(5)	98.7(4)
O(6)-Cu(1)-O(4)	84.6(4)	O(6)-Cu(1)-O(5)	96.8(5)
N(9)-Cu(1)-N(1)	95.2(4)	O(4)-Cu(1)-O(5)	94.4(4)
O(6)-Cu(1)-N(1)	161.5(4)	O(14)-Cu(3)-O(44)	91.0(4)
O(41)-Cu(2)-N(4)	162.8(7)	N(5)#1-Cu(3)-O(44)	82.1(4)
N(2)-Cu(2)-N(4)	95.2(4)	N(6)-Cu(3)-O(44)	177.0(4)
O(8)-Cu(2)-N(4)	81.7(4)	O(14)-Cu(3)-O(15)	91.5(5)
O(41)-Cu(2)-O(7)	91.7(7)	N(5)#1-Cu(3)-O(15)	89.9(4)
N(2)-Cu(2)-O(7)	94.9(4)	N(6)-Cu(3)-O(15)	96.8(4)
O(8)-Cu(2)-O(7)	90.8(4)	O(44)-Cu(3)-O(15)	84.9(4)
N(4)-Cu(2)-O(7)	102.5(5)	O(14)-Cu(3)-N(6)	91.4(4)
O(14)-Cu(3)-N(5)#1	172.8(4)	N(5)#1-Cu(3)-N(6)	95.5(4)

Symmetry transformations used to generate equivalent atoms: #1 -x+1, -y-1, -z.

Table S10. Selected bond lengths [Å] and angles [deg] for **5**

Cu(1)-O(26)	2.299(19)	N(2)-Cu(1)#1	1.965(19)
Cu(1)-N(2)#1	1.965(18)	O(3)-Cu(1)	1.990(17)
O(25)-Cu(1)	1.971(18)	N(1)-Cu(1)	2.005(18)
N(2)#1-Cu(1)-O(25)	93.0(7)	N(2)#1-Cu(1)-O(3)	173.8(8)
O(25)-Cu(1)-O(26)	93.9(8)	N(2)#1-Cu(1)-N(1)	95.7(7)
O(3)-Cu(1)-O(26)	93.6(8)	O(25)-Cu(1)-N(1)	169.5(7)
N(1)-Cu(1)-O(26)	91.6(7)	O(3)-Cu(1)-N(1)	81.4(7)
N(2)#1-Cu(1)-O(26)	91.9(8)	O(25)-Cu(1)-O(3)	89.4(7)

Symmetry transformations used to generate equivalent atoms: #1 -x+3/2, -y-1/2, -z.

Table S11. Selected bond lengths [Å] and angles [deg] for **6**

N(2)-Cu(1)#1	1.94(3)	Cu(1)-N(1)	2.01(3)
Cu(1)-O(2W)	2.40(5)	Cu(1)-O(100)	1.97(2)
Cu(1)-O(1W)	1.95(3)	Cu(1)-N(2)#1	1.94(3)
O(100)-Cu(1)-N(1)	80.5(11)	O(1W)-Cu(1)-O(100)	91.1(12)
O(1W)-Cu(1)-N(1)	171.6(12)	N(2)#1-Cu(1)-N(1)	96.1(12)
N(1)-Cu(1)-O(2W)	83.8(15)	N(2)#1-Cu(1)-O(100)	175.2(13)
O(100)-Cu(1)-O(2W)	92.3(17)	N(2)#1-Cu(1)-O(1W)	92.3(13)
O(1W)-Cu(1)-O(2W)	95.7(17)	N(2)#1-Cu(1)-O(2W)	90.7(18)

Symmetry transformations used to generate equivalent atoms: #1 -x+1, -y, -z+1.

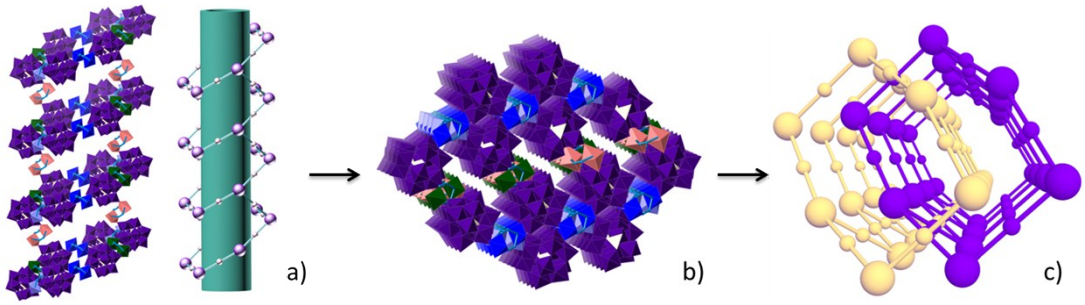

Figure S6. (a) The open channel in complex **1**. (b) Two-fold interpenetrated channels. (c) Topology view of two-fold interpenetrated channels.

Analyses of IR Spectra and PXRD.

The IR spectra of complexes **1–6** are shown in Figure S2–7. The IR spectra exhibit the characteristic peaks at 1015, 971, 923 and 803 cm^{-1} in **1**, 1015, 973920 and 795 cm^{-1} in **5,** 1062, 960, 880, 807 cm^{-1} in **6**, which are attributed toν(Si–O), ν(W=Ot), ν_{as}(W–Ob–W) and ν_{as}(W–Oc–W) from SiW_{12} clusters. The IR spectra exhibit the characteristic peaks at 1061, 962, 882 and 808 cm^{-1} in **2**, 1060, 960, 869 and 803 cm^{-1} in **3**, which are attributed toν(P–O), ν(Mo=Ot), ν_{as}(Mo–Ob–Mo) and ν_{as}(Mo–Oc–Mo) from PMo_{12} clusters. The IR spectra exhibit

the characteristic peaks at 1059, 956, 886 and 818 cm^{-1} in **4**, which are attributed to ν(P–O), ν(W=Ot), ν_{as}(W–Ob–W) and ν_{as}(W–Oc–W) from PW_{12} clusters. Additionally, the bands in the region of 1675 to 1125 cm^{-1} could be ascribed to the characteristic peaks of tda ligands in complexes **1–6**.

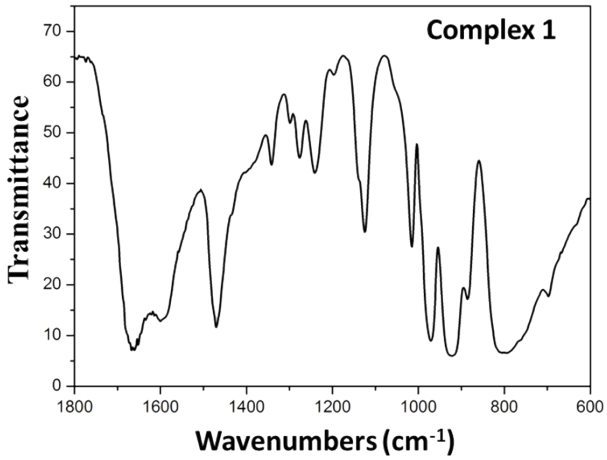

Figure S7. Reflect-IR of complex **1**

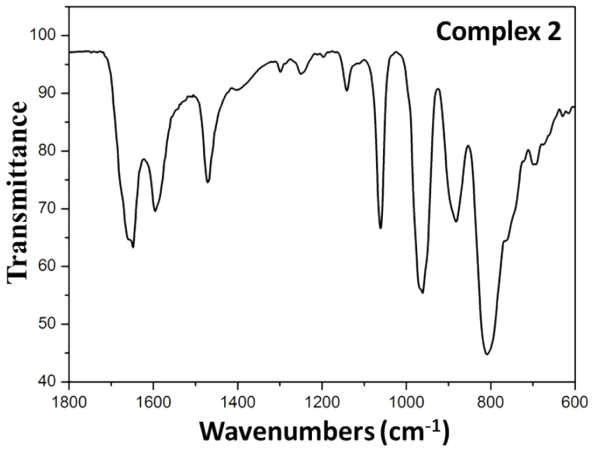

Figure S8. Reflect-IR of complex **2**

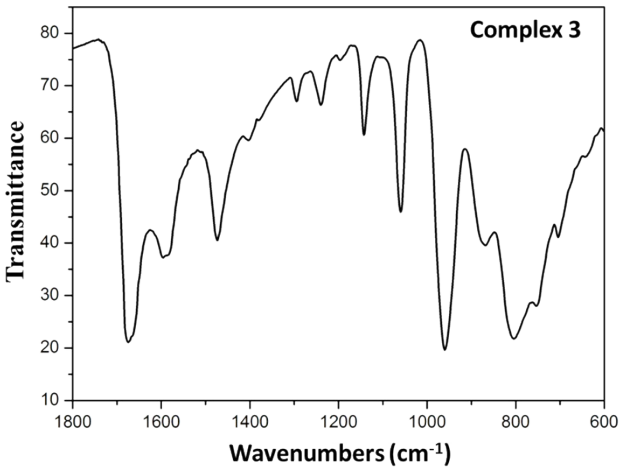

Figure S9. Reflect-IR of complex **3**

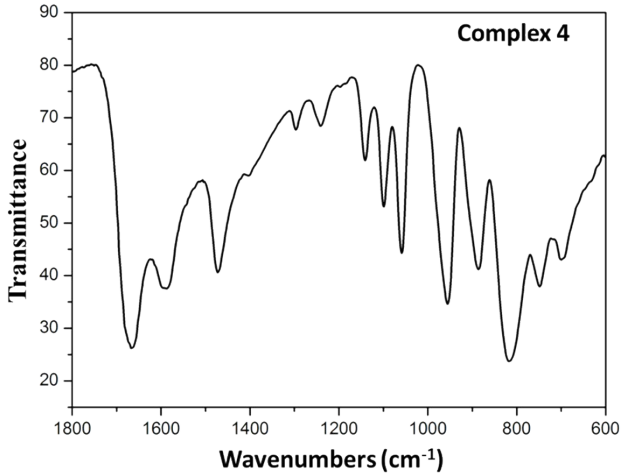

Figure S10. Reflect-IR of complex **4**

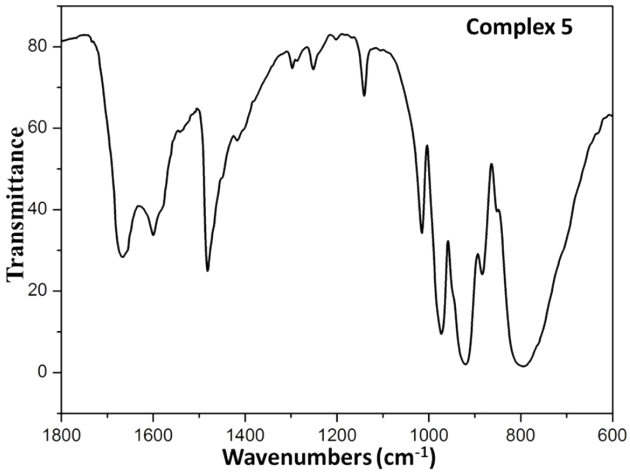

Figure S11. Reflect-IR of complex **5**

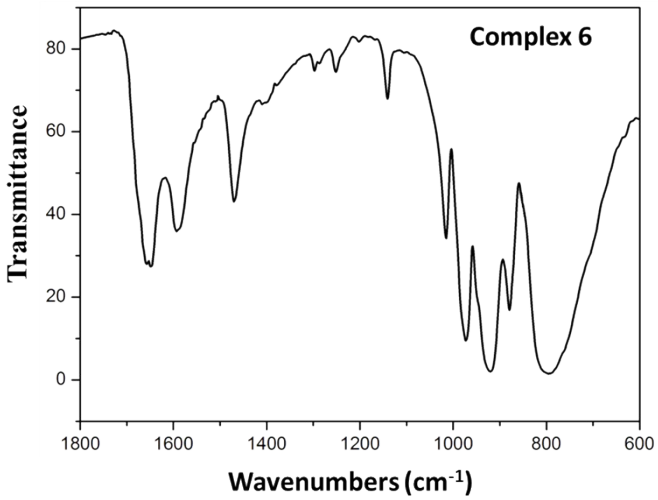

Figure S12. Reflect-IR of complex **6**

Analyses of PXRD.

As shown in Figure S8–13 the X-ray powder diffraction patterns measured for the as-synthesized samples of **1–6** are all in good agreement with the PXRD patterns simulated from the respective single-crystal X-ray data, proving the purity of the bulk phases.

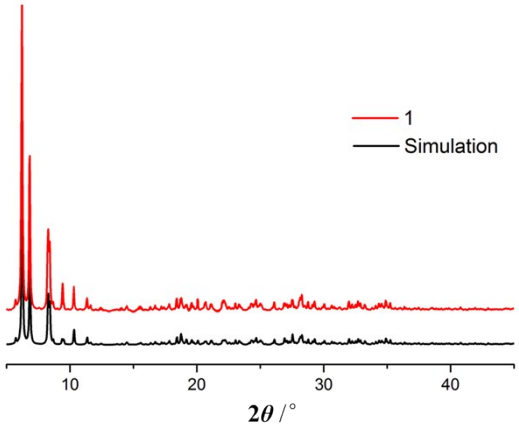

Figure S13. Powder X-ray diffraction patterns for **1**.

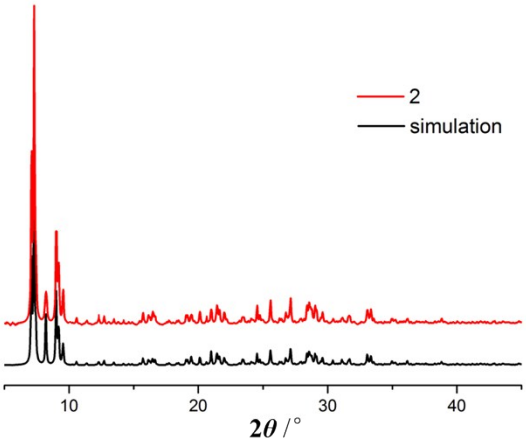

Figure S14. Powder X-ray diffraction patterns for **2**.

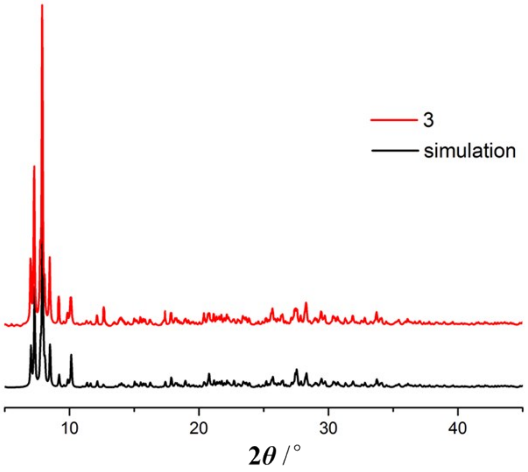

Figure S15. Powder X-ray diffraction patterns for **3**.

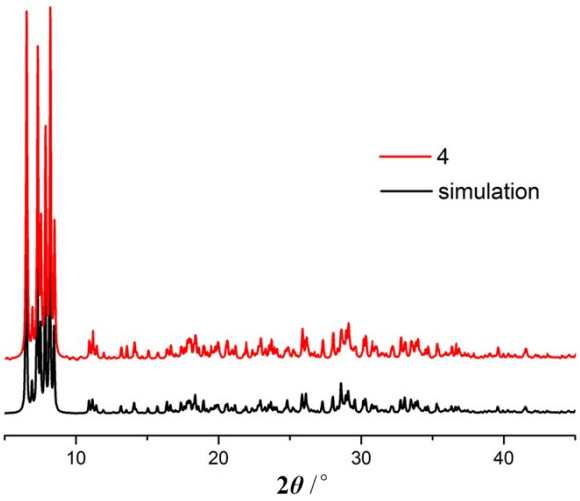

Figure S16. Powder X-ray diffraction patterns for **4**.

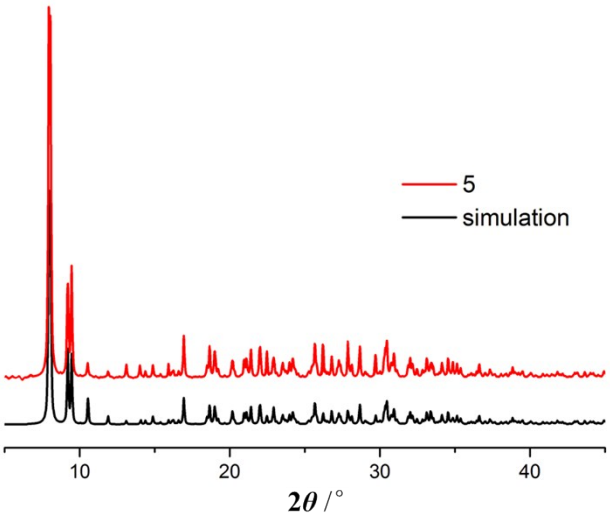

Figure S17. Powder X-ray diffraction patterns for **5**.

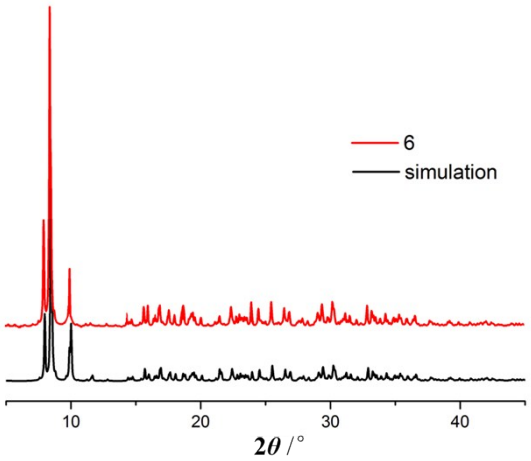

Figure S18. Powder X-ray diffraction patterns for **6**.

PXRD of complexes 1, 5 and 6 before and after the catalytic process.

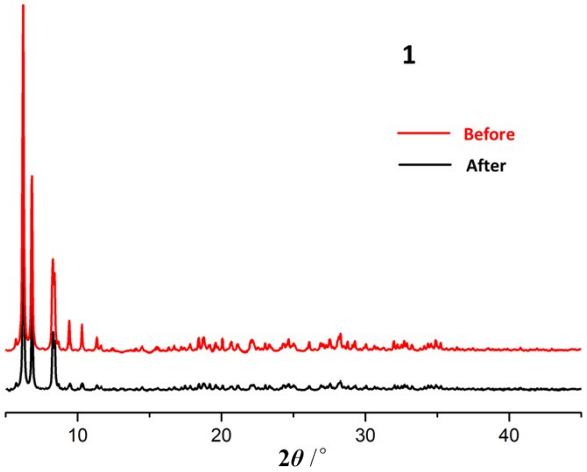

Figure S19. PXRD pattern of complex **1** before (red line) and after (black line) catalytic process.

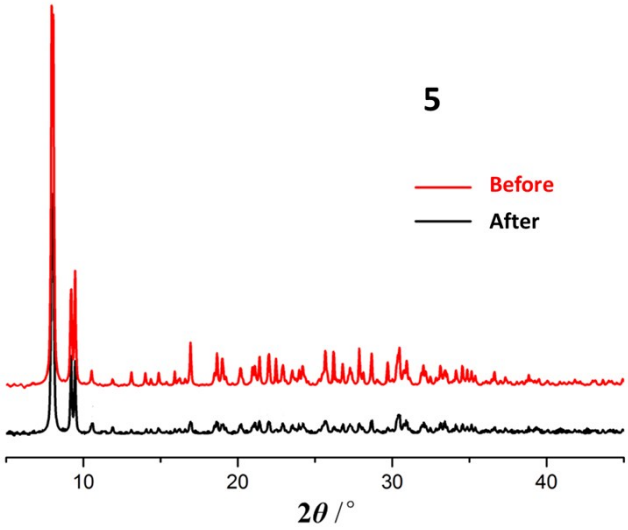

Figure S20. PXRD pattern of complex **5** before (red line) and after (black line) catalytic process.

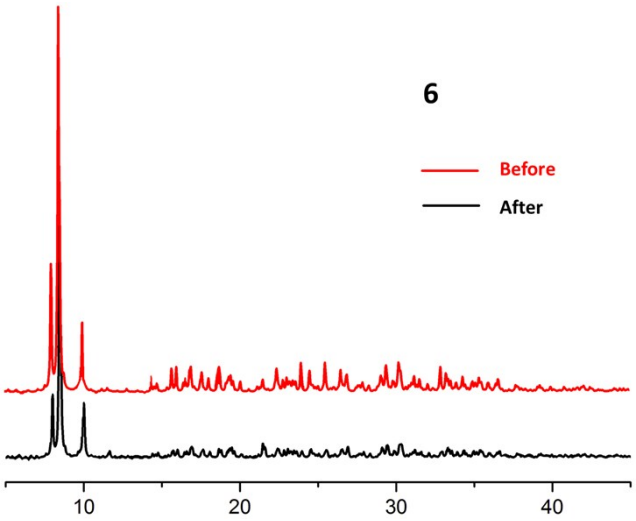

Figure S21. PXRD pattern of complex **6** before (red line) and after (black line) catalytic process.

Thermal Stability of Complexes 1-6.

The thermogravimetric curve for **1** exhibits an initial weight loss of 8.0% before 150 °C, corresponding to the removal of seventeen free and coordinated water molecules (calcd. 7.5%) (Figure S14). After the loss of all the water molecules, the framework begins to decompose with a continuous weight loss up to 250 °C. The TGA curve of **2** shows a weight loss of 7.0% before 280 °C, ascribed to the release of ten water molecules (calcd. 6.7%) (Figure S15). After the loss of all the water molecules, the framework begins to decompose with a continuous weight loss up to 400 °C. In **3**, the result shows a weight loss of 10% during the first major step before 150 °C, corresponding to the removal of fourteen water molecules (calcd. 8.3%) (Figure S16), After the loss of all the water molecules, the framework is stable up to 300 °C and then begins to decompose upon further heating. For **4**, the first weight loss is approximately 12% before 250 °C, attributed to the release of twenty water molecules (calcd. 11.4%) and the framework begins to decompose with a continuous weight loss up to 300 °C (Figure S17). TGA of **5** shows a weight loss of 7.6% around 300 °C which can be assigned due to the loss of four seven molecules and two TMA^+ cations (calc. 6.8%) (Figure S18). After 300 °C the framework begins to decompose. TGA of **6** shows a weight loss of 6.9% around 300 °C which can be assigned due to the loss of four water molecules and two TMA^+ cations (calc. 7.2%) (Figure S19). After 300 °C the framework begins to decompose.

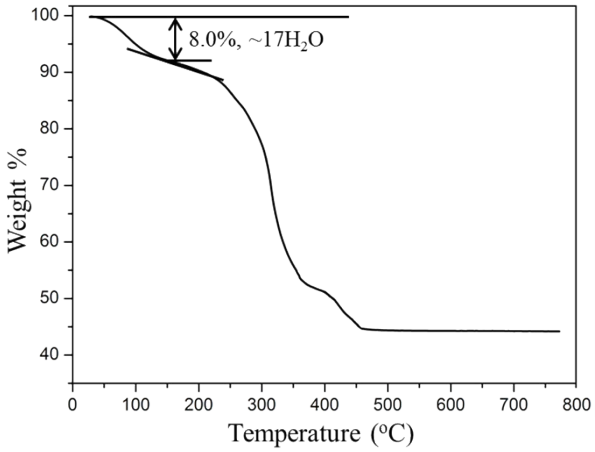

Figure S22. TGA spectra for **1** for the as-synthesized. <150 °C, Loss of surface/free water and coordinated water; >150 °C, framework degradation.

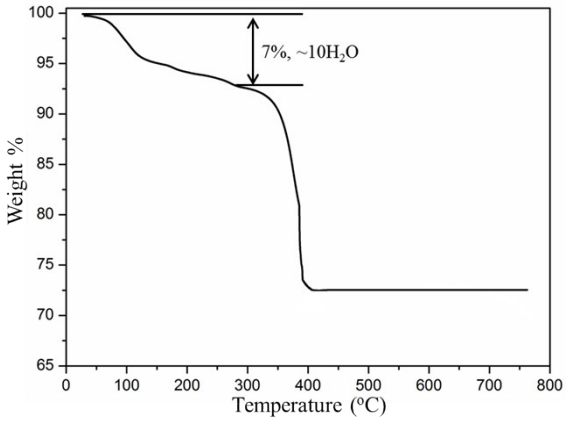

Figure S23. TGA spectra for **2** for the as-synthesized. <280 °C, Loss of surface/free water and coordinated water; >280 °C, framework degradation.

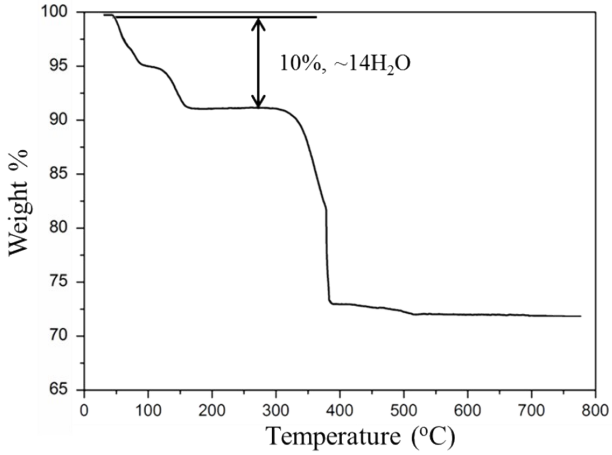

Figure S24. TGA spectra for **3** for the as-synthesized. <300 °C, Loss of surface/free water and coordinated water; >300 °C, framework degradation.

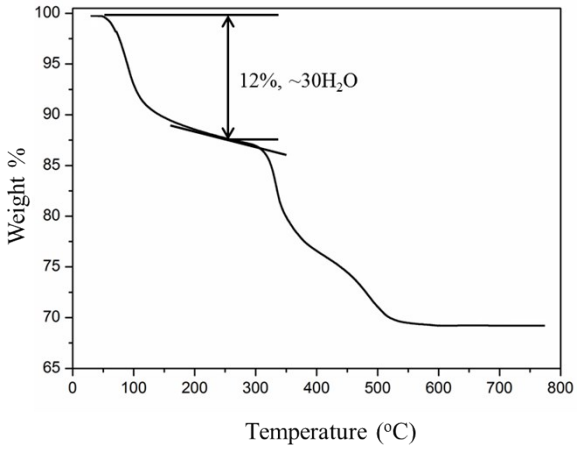

Figure S25. TGA spectra for **4** for the as-synthesized. <250 °C, Loss of surface/free water and coordinated water; >250 °C, framework degradation.

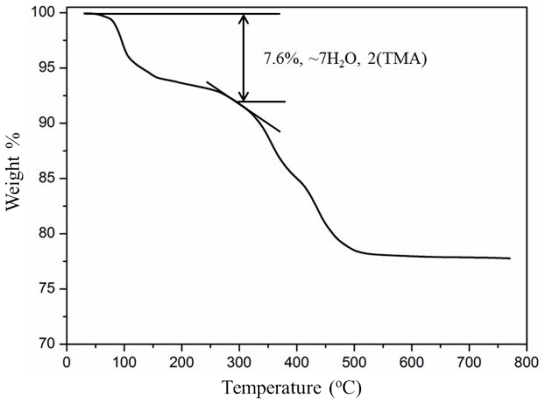

Figure S26. TGA spectra for **5** for the as-synthesized. <280 °C, Loss of surface/free water and coordinated water; >280 °C, framework degradation.

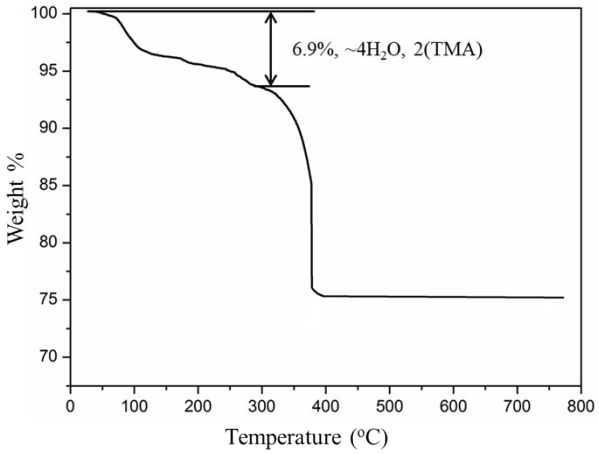

Figure S27. TGA spectra for **6** for the as-synthesized. <300 °C, Loss of surface/free water and coordinated water; >300 °C, framework degradation.